HybriD3 Local Training Scaffold Test

Date: 2026-05-30

PDF version: hybrid3-local-training-scaffold-test.pdf

Summary

This local smoke study pulled ten similar HybriD3 atomic-structure records, cataloged their database and crystallographic metadata, generated a compact GIWAXS simulation set for 2D fibril-textured samples, applied detector-image artifacts, trained the baseline vector ranker, evaluated top-k recovery, and exported ranked structure-file guesses.

Quantity	Value
Structures pulled	10
Clean simulation samples	20
Artifact-augmented samples	80
Missing-wedge corrected clean samples	20 / 20
Median missing-wedge masked fraction	0.082
Surface-artifact augmented samples	60
Ranker candidates	20
Evaluated artifact images	80
Solvable augmented fraction	1.000
Median artifact SNR	13.49
Top-1 accuracy	0.988
Top-5 accuracy	1.000

Pulled Structure Cohort

Selection targeted visible HybriD3 atomic-structure datasets with 2D `PbI4` lead-iodide inorganic sublattices. This gives a chemically coherent local test set for fibril-textured GIWAXS recognition while keeping the run small.

Dataset	Structure id	Inorganic	Organic	File	Sites
2788	`hybrid3_2788`	PbI4	C4H9NI	`dataset_2788_20231011_MC3I_PbI_380K_red.cif`	20
2787	`hybrid3_2787`	PbI4	C4H9NI	`dataset_2787_20250421_MC3I_PbI_360K_1_red.cif`	20
2786	`hybrid3_2786`	PbI4	C4H9NI	`dataset_2786_MC3PI_100K.cif`	20
2736	`hybrid3_2736`	PbI4, Lead iodide	C7H9IN	`dataset_2736_geometry.vasp`	82
2735	`hybrid3_2735`	PbI4, Lead iodide	C7H9BrN	`dataset_2735_geometry.vasp`	82
2734	`hybrid3_2734`	PbI4, Lead iodide	C7H9ClN	`dataset_2734_geometry.vasp`	82
2733	`hybrid3_2733`	PbI4, Lead iodide	C7H9FN	`dataset_2733_geometry.vasp`	164
2732	`hybrid3_2732`	PbI4, Lead iodide	C6H18N2	`dataset_2732_geometry.vasp`	62
2731	`hybrid3_2731`	PbI4, Lead iodide	C8H22N2	`dataset_2731_geometry.vasp`	74
2730	`hybrid3_2730`	PbI4, Lead iodide	C2H8NO	`dataset_2730_geometry.vasp`	58

Simulation Protocol

Clean GIWAXS images were generated on a deliberately lower-information reciprocal-space grid with `qxy = [-2.8, 2.8] A^-1`, `qz = [0.0, 2.8] A^-1`, and `160 x 128` local smoke-test pixels. The default cap is now biased toward 2-3 A^-1 rather than 4 A^-1 so the solver is tested against detector windows that resemble practical GIWAXS measurements with less high-q information. The texture model was `fiber_gaussian` with `theta_x = 90 deg`, `theta_y = 0/90 deg`, `sigma_theta = 0.035`, `sigma_phi = 0.28`, `sigma_r = 0.04`, q-dependent broadening terms of `0.25` in-plane and `0.15` out-of-plane, and `hkl_extent = 14`. The hkl extent is selected as the maximum recommended reciprocal-lattice search across the pulled structures for the requested q-range, so long-axis 2D structures such as `hybrid3_2788`, `hybrid3_2787`, and `hybrid3_2786` still populate the detector plane out to `q <= 2.8 A^-1`.

The local forward model now includes a first-order flat-detector solid-angle response derived from the Ewald-sphere scattering angle `q = 4 pi sin(theta) / lambda`. This keeps the edge of the detector realistic while preserving the existing labeled `(hkl)` peak table contract. The same incident-angle geometry is also applied as a pyFAI-style fiber/GI missing-wedge correction in qIP/qOOP space, so inaccessible bins below the sample horizon are zeroed and excluded from the labeled `(hkl)` peak table. This run applied the `pyfai_fiber_qip_qoop_accessibility` missing-wedge model to 20 of 20 clean samples, with a median horizon of `qz = 0.0219 A^-1` and a median masked fraction of 0.082. Every generated clean label stores a `simulation_metadata` block with the missing-wedge model, incident angle, wavelength, horizon, and masked fraction used for the example.

Detector artifacts were generated from the scaffold artifact profiles: `clean`, `default`, `harsh_detector`, and `pilatus1m_reference`. Diffuse scattering is now generated as broad rings centered on q-values inferred from the simulated Bragg signal, instead of arbitrary vertical detector streaks. The profiles also include Poisson noise, Gaussian read noise, q-dependent background, direct/specular beam artifacts, Yoneda bands, substrate horizon shadowing, critical-angle peak splitting, beamstop shadow, flat-field variation, hot/dead pixels, dead-pixel clusters, saturation, and detector-module masks scaled from randomized common detector footprints including PILATUS 1M, EIGER2, and a continuous PerkinElmer-style flat panel. The direct-beam, Yoneda, horizon, and critical-angle operators use the same incident angle and wavelength stored in the detector geometry. The critical angle is estimated from the parsed structure electron density unless a profile overrides it. The substrate horizon model computes beam-footprint spillover from substrate dimensions, beam width/height, and incident angle, then uses that spillover to tune the horizon shadow, below-horizon leakage, and added qz peak broadening. The active surface-scattering operations in this example are `direct_beam_specular`, `yoneda_band`, `critical_angle_peak_splitting`, `substrate_horizon_shadow`, `footprint_spillage_peak_broadening`. Each artifacted label now includes an `artifact_assessment` block that turns direct beam, specular reflection, Yoneda bands, substrate horizon/footprint spillage, critical-angle peak splitting, beamstop shadows, and detector masks into compact q-space or pixel-space regions. The feedback evaluator and exported structure guesses rasterize those regions into artifact-aware ranking weights and blend them with the clean image-overlap score, so non-Bragg aberrations are recognized without discarding the Bragg-rich regions needed for peak assessment/indexing tests.

The mathematical surface-artifact contract and artifact-aware training model are documented in Surface Artifacts And Training Model.

The augmentation quality gate records `quality_assessment` for every label. In this smoke run, 80 of 80 artifacted samples are marked solvable, with a median signal-to-noise of 13.49 and a median retrievable-signal fraction of 1.000. The harsh profile is kept as a controlled stress-test tail, but its noise, saturation, horizon spillover, direct-beam, and diffuse-ring strengths are bounded so it remains a recoverable indexing problem rather than an unrealistic failure case.

Simulation Examples

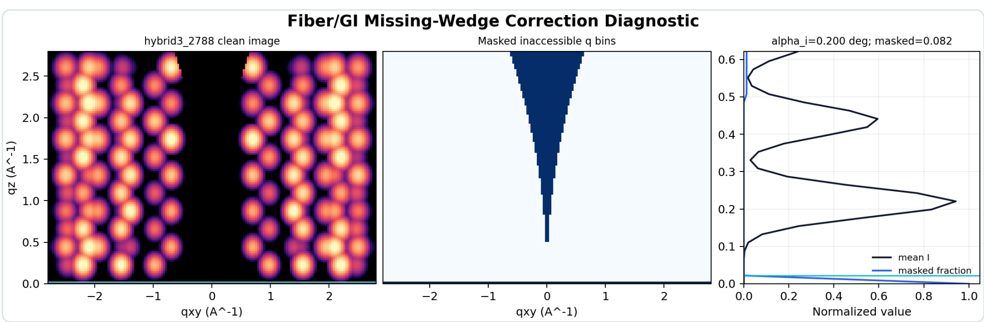

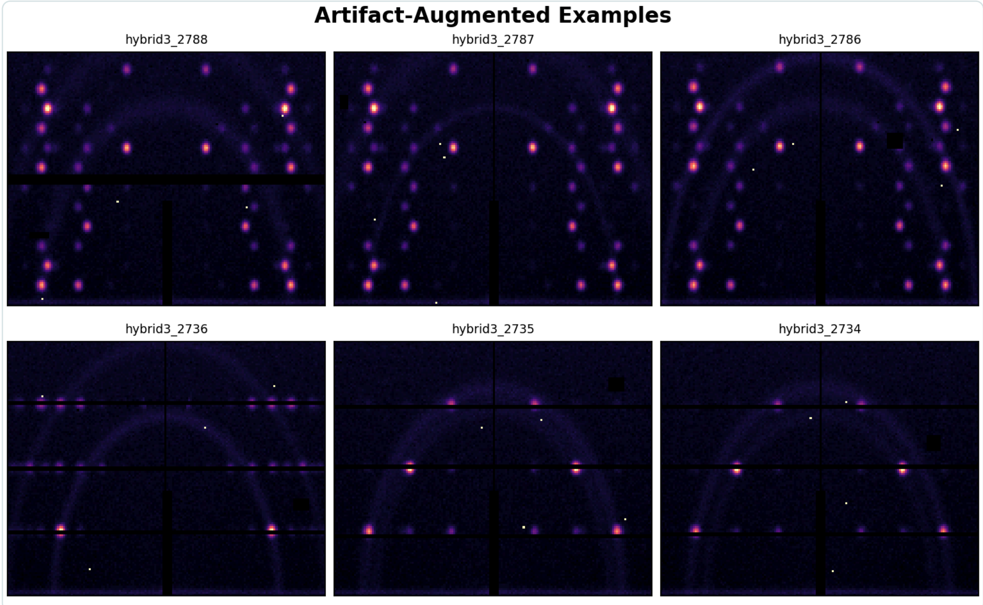
Artifact-Augmented Examples
hybrid3_2788
hybrid3_2787
hybrid3_2786
hybrid3_2736
hybrid3_2735
hybrid3_2734

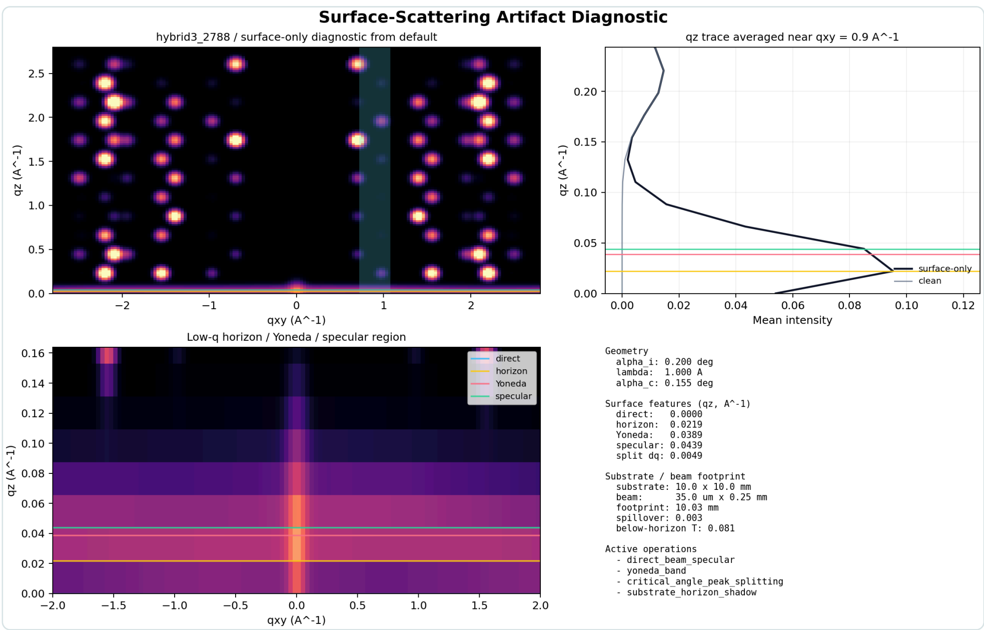
Surface-Scattering Artifact Diagnostic
hybrid3_2788 / surface-only diagnostic from default
qz (A^-1)
qxy (A^-1)
qz trace averaged near qxy = 0.9 A^-1
Mean intensity
surface-only
clean
Low-q horizon / Yoneda / specular region
direct
horizon
Yoneda
specular
Geometry
alpha_i: 0.200 deg
lambda: 1.000 A
alpha_c: 0.155 deg
Surface features (qz, A^-1)
direct: 0.0000
horizon: 0.0219
Yoneda: 0.0389
specular: 0.0439
split dq: 0.0049
Substrate / beam footprint
substrate: 10.0 x 10.0 mm
beam: 35.0 um x 0.25 mm
footprint: 10.03 mm
spillover: 0.003
below-horizon T: 0.081
Active operations
- direct_beam_specular
- yoneda_band
- critical_angle_peak_splitting
- substrate_horizon_shadow

Output Locations

Output	Path
Run root	`/Users/keithwhite/repos/ewald/data_training/runs/hybrid3_2d_fibril_smoke_20260530`
HybriD3 catalog	`/Users/keithwhite/repos/ewald/data_training/runs/hybrid3_2d_fibril_smoke_20260530/hybrid3_library/hybrid3_str`
Ingest manifest	`/Users/keithwhite/repos/ewald/data_training/runs/hybrid3_2d_fibril_smoke_20260530/hybrid3_library/hybrid3_ing`
Clean simulation manifest	`/Users/keithwhite/repos/ewald/data_training/runs/hybrid3_2d_fibril_smoke_20260530/simulations/manifest.jsonl`
Artifact manifest	`/Users/keithwhite/repos/ewald/data_training/runs/hybrid3_2d_fibril_smoke_20260530/artifacts/artifact_manifest`
Ranker model	`/Users/keithwhite/repos/ewald/data_training/runs/hybrid3_2d_fibril_smoke_20260530/model/vector_ranker.json`
Feedback metrics	`/Users/keithwhite/repos/ewald/data_training/runs/hybrid3_2d_fibril_smoke_20260530/metrics/feedback_metrics.js`
Exported guesses	`/Users/keithwhite/repos/ewald/data_training/runs/hybrid3_2d_fibril_smoke_20260530/structure_guesses`

Testing Protocol

1. Verify HybriD3 REST access and select ten visible 2D `PbI4` atomic-structure datasets.
2. Download structure-like files from HybriD3 dataset pages and JSmol media endpoints.
3. Convert supported structure variants to simulator-readable CIF/POSCAR files.
4. Write an enriched EWALD structure catalog with API metadata and file-derived crystallographic metadata.
5. Generate clean GIWAXS simulations using the 2D fibril-texture sweep and verify the `simulation_metadata.missing_wedge_correction_applied` labels.
6. Apply deterministic detector and surface-scattering artifacts, then verify `artifact_metadata.operations`, `artifact_assessment.regions`, and `quality_assessment`.
7. Build the baseline vector-ranker checkpoint from clean simulations.
8. Evaluate artifact images against the ranker and export top-k structure-file guesses for downstream structure-analysis testing.

Detector And Literature Basis

- The PILATUS 1M reference mask follows published modular-detector behavior: the original 18-module detector has a large pixel array, module gaps, and measurable non-responding pixels that must be masked or treated during data reduction.
- The pyFAI detector database provides practical detector definitions and masks for many common X-ray detectors, including PILATUS, EIGER, PerkinElmer, Rayonix, Lambda, Jungfrau, and other beamline detector families.
- The EIGER2 detector profiles use the DECTRIS-published 75 um pixel size and inter-module gap patterns for EIGER2 X detector geometries.
- The GIWAXS protocol follows the perovskite-oriented guidance in Steele et al., "How to GIWAXS: Grazing Incidence Wide Angle X-Ray Scattering Applied to Metal Halide Perovskite Thin Films," Advanced Energy Materials 2023, 13, 2300760, including attention to q-range, grazing-incidence geometry, detector mapping, and orientation-sensitive interpretation.

References:

- Broennimann et al., "The PILATUS 1M detector," https://journals.iucr.org/s/issues/2006/02/00/gf0003/
- pyFAI detector distortion and detector-definition documentation, https://pyfai.readthedocs.io/en/latest/usage/tutorial/Detector/Distortion/Distortion.html
- DECTRIS EIGER2 X/XE detector specifications, https://www.dectris.com/en/detectors/x-ray-detectors/eiger2/eiger2-for-synchrotrons/eiger2-x/
- Steele et al., Advanced Energy Materials 2023, DOI 10.1002/aenm.202300760, https://doi.org/10.1002/aenm.202300760

Interpretation

This is a scaffold validation, not a final scientific model benchmark. The baseline vector ranker is intentionally simple: it tests whether the data contracts, labels, manifests, image generation, artifact augmentation, and structure-guess export are connected. The next technical step is to replace the baseline ranker with a learned peak-detection/indexing/retrieval model while keeping the same manifest and reporting contracts.